Ultrafast Condensed Matter Physics at Attoseconds

Shi-Qi Hu(胡史奇)[1] and Sheng Meng(孟胜)[1,2,3*]

[1]*Beijing National Laboratory for Condensed Matter Physics and Institute of Physics, Chinese Academy of Sciences, Beijing 100190, China*
[2]*School of Physical Sciences, University of Chinese Academy of Sciences, Beijing 100049, China*
[3]*Songshan Lake Materials Laboratory, Dongguan 523808, China*

(Received 10 October 2023; accepted manuscript online 19 October 2023)

Our understanding of how photons couple to different degrees of freedom in solids forms the bedrock of ultrafast physics and materials sciences. In this review, the emergent ultrafast dynamics in condensed matter at the attosecond timescale have been intensively discussed. In particular, the focus is put on recent developments of attosecond dynamics of charge, exciton, and magnetism. New concepts and indispensable role of interactions among multiple degrees of freedom in solids are highlighted. Applications of attosecond electronic metrology and future prospects toward attosecond dynamics in condensed matter are further discussed. These pioneering studies promise future development of advanced attosecond science and technology such as attosecond lasers, laser medical engineering, and ultrafast electronic devices.

DOI: 10.1088/0256-307X/40/11/117801

1. Introduction. Atomic structures and surrounding electrons determine properties of a material. Understanding and manipulating electrons, nuclei, and various quasiparticles as well as interactions between them in materials have become one of the core tasks of contemporary condensed matter physics and materials science. Since the invention of laser in 1960s,[1] light-induced ultrafast dynamics has acted as a new approach to explore and modulate properties of condensed matter, alongside with other compensating factors including temperature, pressure, magnetic field, and strain. Significant progresses have been made in these fast-evolving fields, and there are examples including light-induced room temperature superconductivity,[2,3] laser-induced anomalous Hall effect in graphene,[4] and nonthermal manipulation for hidden states in solids (such as novel charge density waves (CDWs)[5–7] and Floquet engineering[8,9]).

Along with these great achievements, more challenges arise, including dynamic description on the formation of polaron and Cooper pairs, the mechanisms behind high-temperature superconductivity, accurate quantification of spin exchange interaction, and electron screening effects. In these processes, electron dynamics always plays a crucial role. Therefore, solutions to these scientific and technological problems will require insight into more fundamental problems, as pointed by the 2022 Wolf Prize winners, Paul Corkum, Anne L'Huillier, and Ferenc Krausz in an interview:[10] "How do electrons interact with each other inside solid matter? What is the ultimate time response of electronic matter?"

Considering that the intrinsic temporal and spatial scale of electron dynamics lies at the attosecond (as, $1\,\text{as} = 10^{-18}$ s) and picometer (pm, $1\,\text{pm} = 10^{-12}$ m) scales, for example, the ground state orbital radius of the hydrogen atom is ~ 53 pm, while the period of electron motion around the hydrogen nucleus is ~ 152 as, attosecond physics with ultrahigh temporal and spatial resolutions is urgently needed in order to solve the above significant challenges. Most recently, Pierre Agostini, Ferenc Krausz, and Anne L'Huillier are awarded the 2023 Nobel Prize in Physics for their ground-breaking works to experimentally generate the attosecond pulses of light for the study of electron dynamics in matter.

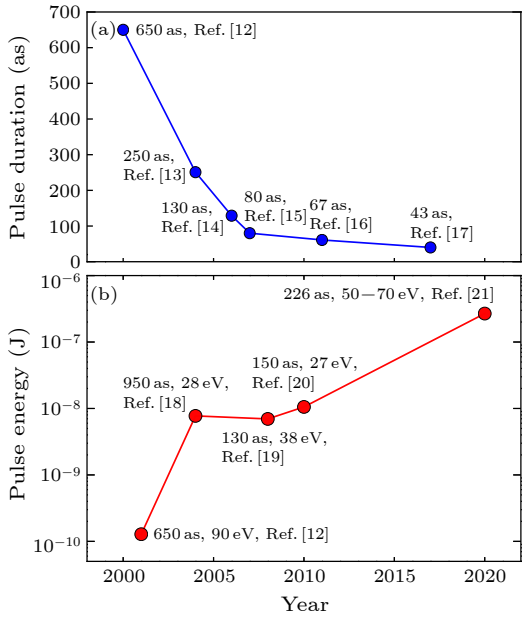

Fig. 1. Representative results in the progress of pulse duration (a) and pulse energy (b) of attosecond pulses.

Attosecond condensed matter physics, which describes the science of atomic scale electronic motions in condensed

*Corresponding author. Email: smeng@iphy.ac.cn

matter at a scale of a few to hundreds of attoseconds, has become an essential research hotspot in the fields of fundamental physics, optoelectronics and semiconductor devices, solar cell industry, and even biochemical reactions in living systems. The exploration of attosecond dynamics in these fields has in turn driven development of advanced technologies[11] such as ultra-short[12–17] and ultra-strong laser pulses[12,18–21] (pulse duration about tens of attosecond, and the pulse energy ~ 250 nJ, as shown in Fig. 1).

In this review, the latest developments in attosecond dynamics of condensed matter are summarized. We first refer to the spectroscopy metrology and imaging technology with the attosecond resolution, and then focus on the attosecond dynamics of charge, exciton, and magnetism in solids with several representative examples. The significant concept and indispensable role of interactions among multiple degrees of freedom [e.g., electron–electron (e–e) correlations, electron–hole (e–h) interactions, spin–orbital couplings (SOC), and electron–phonon couplings (EPC)] in solids are explained and highlighted (as shown in Fig. 2), followed by the application of attosecond dynamics in electronic devices and information technology. Future prospects of attosecond dynamics in condensed matter are further discussed.

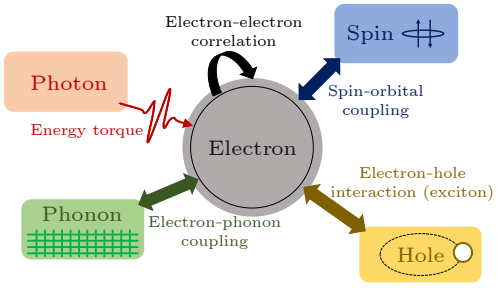

Fig. 2. Schematic of multiple reservoirs and quasiparticle interactions for the ultrafast dynamics in solids.

2. Attosecond Spectroscopy and Imaging Techniques. To detect and track the attosecond dynamics in condensed matter, one needs the probe with: (i) sufficient time resolution to distinguish the electron-interaction-imposed changes in real time; (ii) sensibility to the complex states/phases and abundant many-body interactions in solids; and (iii) compatibility to different environments.

In the past decades, the discovery of high harmonics with extreme ultraviolet (XUV) radiation and synchronized beams enables the attosecond pulse generation with tens of attosecond duration[22] and a wide frequency range spectroscopy from terahertz (THz) to ~ 100 petahertz (PHz) and even beyond. These great milestones on laser technology, with the pump-probe setup, provide powerful spectroscopies [including the high harmonic generation spectroscopy, the attosecond transient absorption/reflection spectroscopy (ATAS/ATRS), and the attosecond photoelectron spectroscopy (APS)] for users in ultrafast community to get insight into the time window of the very first response following light–matter interaction and the ultrafast changes in the electronic states, from which different degrees of freedom coupled with light can be thus disassembled.

On the other hand, the broadband spectrum not only provides the simultaneous probing of multiple electronic states, but also enables their transitions as a reporter of element-specific electronic or spin properties. More details on these spectroscopies are well reviewed in recent literature.[23–25]

Moreover, by combining with attosecond laser pulse as well as the pump-probe setup, researchers also equipped conventional imaging techniques with the attosecond resolution, realizing the attosecond scanning tunnelling microscopy (ASTM) and the attosecond transmission electron microscopy (ATEM).

High Harmonic Generation Spectroscopy. High harmonic generation (HHG), the process of generating XUV coherent radiation far higher than the incident photon energy which originates from the nonlinear electron motion within/between electronic states driven by strong-field light–matter interactions,[26,27] naturally contains fingerprints of intrinsic atomic and electronic properties of materials. In the early 2000s, the HHG in solids is first observed in semiconductors ZnS and ZnSe.[28] Later in 2011, HHG beyond the band edge and up to 25$^{\text{th}}$ order has been realized in solids,[29] and a lot of excitements are emerging in the community on learning about the material's properties through HHG spectroscopy, including the band structures,[30–32] electronic topology,[33–35] and lattice symmetry/atomic configuration.[36,37] Via *in situ* phase-sensitive measurements, Vampa *et al.*[30] realized for the first time the all-optical reconstruction of band-gap dispersion in ZnO. Based on the Bloch oscillation picture, Luu *et al.*[33] mapped out the Berry curvature over the entire Brillouin zone of insulator SiO_2. Very recently, using HHG we and our collaborators at Rostock University[37] demonstrated that intense optical fields interacting with solids could enable the imaging of valence electrons in MgF_2 and CaF_2 at the precision of ~ 26 pm [Fig. 3(b)], even though the wavelengths of the photons are about 10^5 times larger than atomic scales. In a subsequent study we further reveal a dynamic imaging of valence electrons in MgF_2 [Fig. 3(c)], where an ultrafast oscillation of valence electron density at the attosecond scale is obtained.[38] The strong laser field continuously transports electrons between Mg and F ions, resulting in a time-dependent orbital distribution of valence electrons as well as the HHG emissions.[38]

Attosecond Transient Absorption/Reflection Spectroscopy. The typical ATAS/ATRS experiments involve the photoexcitation of samples by a UV–visible–IR pump pulse, which is probed by an XUV pulse via core-to-valence electronic transition. In this pump–probe fashion, the transient/reflective change in XUV absorption is measured as a function of time delay between the two pulses.

In the last decade, ATAS/ATRS has been widely applied to investigate various ultrafast dynamics within different field strength regimes. If the field is not so strong, several studies[39,40] explored the multiphoton excitation in GaN and GaAs, the absorption oscillating with a periodicity of 860 as in GaN reveals the optical-driven dipolar oscillation at a frequency of 1.16 PHz. Moreover, the

intraband dynamics in GaAs is revealed to significantly enhance the carrier injection even with resonant excitation. Under strong fields, Schultze *et al.*[41,42] performed the first ATAS experiment in SiO_2 and Si, where the Wannier–Stark localization[43] driven by strong laser field and the band-gap reduction induced by a ~ 450 as carrier tunnelling have been revealed. In the intermediate field situation, Lucchini *et al.*[44] demonstrated the attosecond dynamical Franz–Keldysh effect (DFKE) in diamond.

The technique was further applied[45] to provide an unambiguous and simultaneous view on the temporal evolution of the photon-carrier-phonon system in graphite. As shown in Fig. 3(a), the spectroscopy reveals an ultrafast dephasing along with the impact excitation and Auger heating for carriers, whereas the excitation of strongly coupled A_1' phonons, instead of the common E_{2g} phonons, dominates the dissipation channel of electronic coherence.

Attosecond Photoelectron Spectroscopy. The APS is based on the photoelectric effect, where attosecond photoelectron is generated by photoionization. Another visible or near-infrared (NIR) laser field is used as the streaking field to deflect the photoelectron momentum. By changing the relative delay between two lasers, the photoelectron spectrogram contains information of ultrafast processes such as photoionization delay,[46–48] temporal phase of attosecond pulse,[49] and photoexcited carrier dynamics.[50] The most well-known APS is attosecond streak camera (ASC) and reconstruction of attosecond beatings by interferences of two-photon transitions (RABBITTs).

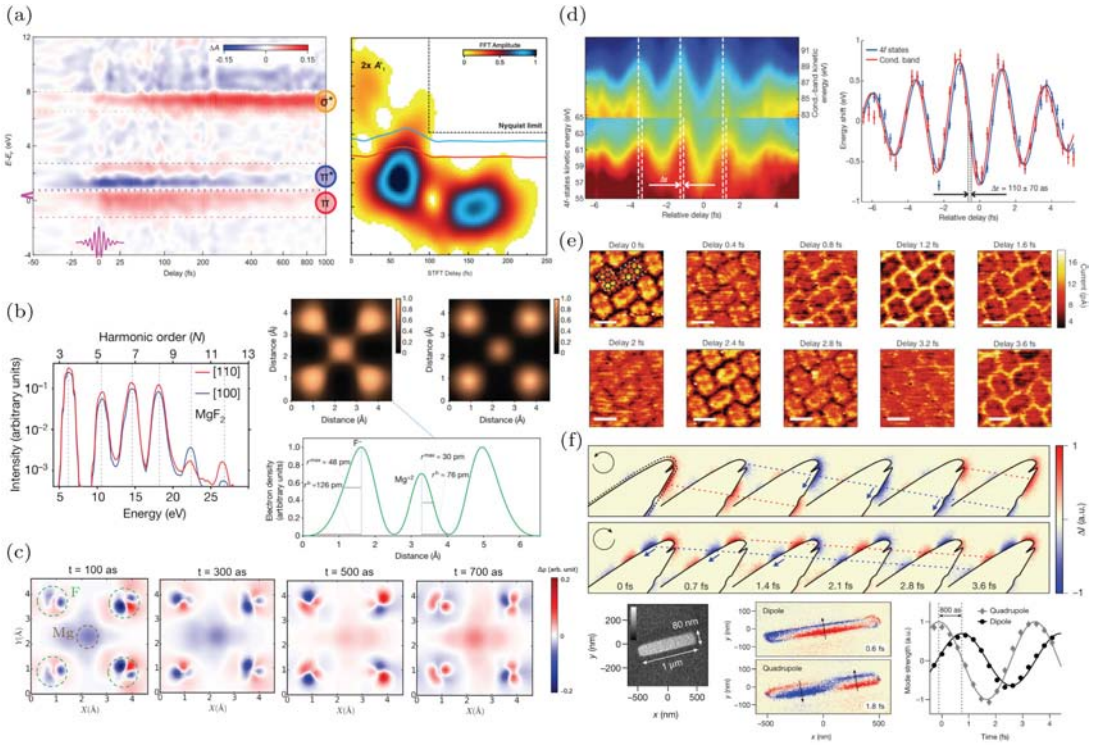

Fig. 3. (a) Time-resolved transient absorption (ΔA) of graphite (left). Short-time Fourier transform spectra performed on ΔA near the σ^* band (right). (b) Harmonic spectra generated in MgF_2 (left). Valence electron density derived from the HHG and DFT simulation of MgF_2 (right). (c) Snapshots of the fluctuations of valence electron density in MgF_2 under strong field. (d) The APS as a function of time for electrons of $4f$ state and conduction band (left). Quantification of the APS shift for electrons of $4f$ state with respect to the conduction band (right). The ~ 100 as delay in emission is illuminated. (e) Spatially resolved laser-induced tunnelling current as a function of the delay between two pulses. (f) Time-resolved electron energy changes for left-circular and right-circular excitation light (top). Snapshots of dipole mode (0.6 fs) and quadrupole mode (1.8 fs) of the slit resonator. Time-dependent strength of the dipole (circles) and the quadrupole (diamonds) from singular-value decomposition of the measured data (bottom). Here, (a) is taken from Ref. [45]; (b), (c), (d), (e), and (f) are taken from Refs. [37,38,51–53], respectively.

In 2007, Cavalieri *et al.*[51] gave the first direct observation of attosecond electron transport by ASC in solid tungsten. The spectroscopy reveals a ~ 100 as delay of emission between the localized $4f$ electrons and delocalized conduction-band electrons [Fig. 3(d)]. Later in 2016, Tao *et al.*[54] combined the RABBITT technology with angle-resolved photoelectron spectroscopy (ARPES) and measured the lifetime of the excited state of Ni(111) to be ~ 200 as, which is strongly dependent on the emission angle and is interpreted as a result of wave function attenuation as well as the band dispersion modulation of the final state. Most recently, Heinrich *et al.*[55] extended the RABBITT technology to deeply bound electronic states and identified the different contributions from *sp* and *d* orbitals. A 39 ± 18 as delay of the photoemission between these orbitals was extracted.

Attosecond Scanning Tunnelling Microscopy and Transmission Electron Microscopy. The above-mentioned

attosecond techniques are able to generate and trace the ultrafast dynamics in real time, but not in real space. By contrast, combining the attosecond techniques with atomic-scale spatial resolution probe is entering the mainstream. By irradiating the tunnel junction with carrier-enveloped, phase-stabilized femtosecond light pulses, Garg and Kern [52] developed the ASTM to directly visualize the electronic coherence on the atomic scale achieving an approximately 200 as resolution. As shown in Fig. 3(e), by tuning the delay between two orthogonally polarized laser and performing space-resolved topographic scans of the laser-induced tunnelling current, they got coherent oscillation of electron density with a period of ~ 2.7 fs, which involves the interference between highest occupied molecular orbital (HOMO) of the adsorbed perylenetetracarboxylic dianhydride molecules and the Au(111) surface state.

Another progress lies in the ATEM recently achieved by Nabben *et al.* [53] They applied a continuous-wave laser to modulate the electron wave function into a rapid sequence of electron pulses, and used an energy filter to resolve electromagnetic near-fields in and around a nanostructure as a movie in spacetime. They investigated the spatiotemporal chirality of the near-fields around a plasmonic needle tip and the spatiotemporal response of dielectric nano-resonators [see Fig. 3(f)]. An oscillation of both quadrupole and dipole modes with a period ~ 3.6 fs is observed, while the two dynamical behaviors are time-shifted by a delay of 800 ± 100 as.

3. Attosecond Dynamics of Solids. Investigations on attosecond dynamics enable researchers to obtain new clues about how a material acquires its function through the interplay among various degrees of freedom over time. This makes up the bedrock of contemporary ultrafast sciences.

Before the emergence of ultrafast condensed matter physics, the attosecond dynamics in atoms and molecules has gained wide attention. [56–61] For example, the pioneering work by Calegari *et al.* [62] figured out the ultrafast charge migration in the phenylalanine with a sub-4.5-fs oscillation after prompt ionization. Soon after, Kraus *et al.* [63] advanced HHG spectroscopy to improve the time resolution up to $\sim$ 100 as, and reconstructed the full quantum charge dynamics in iodoacetylene. Via ATAS, Matselyukh *et al.* [64] investigated the excite-state nonadiabatic (NA) dynamics in SiH_4 molecules with strong nuclear-electron couplings. A 690 as charge migration has been revealed to result from the electronic coherence between the valence and Rydberg excited states. This electronic coherence partially transfers to other states after ~ 40 fs, due to the overlap of nuclear wavepackets and the NA dynamics in the populated Rydberg/valence states.

In contrast, research on attosecond dynamics of solids is in its infancy, since many fundamental issues are still in dispute. In the following we focus on the attosecond dynamics of charge, exciton, and magnetism in solids and highlight the significant roles of many-body interactions in these processes.

Attosecond Charge Dynamics. Previous discussions on the ATAS/ATRS have shown the impact of light–matter interaction on the attosecond dynamic of solids. As the field becomes stronger, charge dynamics in solids undergoes a transition from multiphoton absorption to electron tunnelling. The material functions such as dielectric properties and electron screening are modulated correspondingly.

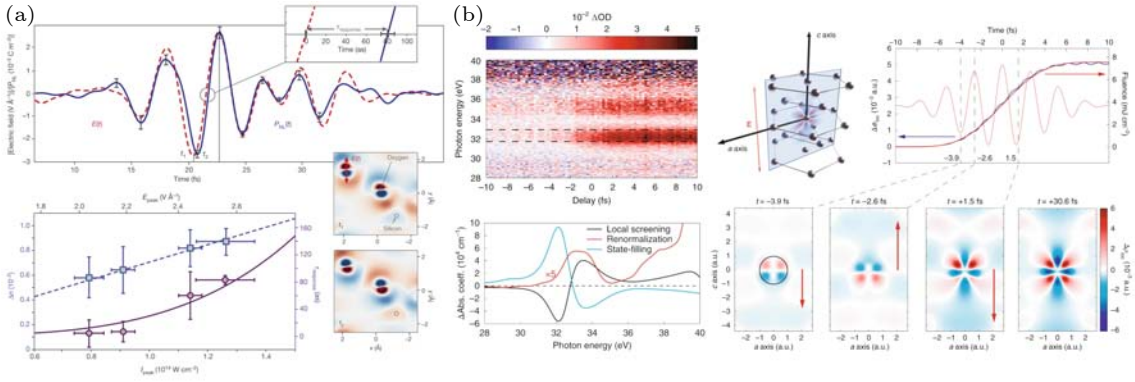

Fig. 4. (a) The electric field back-propagated of fused silica is contrasted with the nonlinear polarization (NP) evaluated from laser field (top). The response time of the NP is found to be ~ 100 as. The insets display the electron density distribution for two extrema of the electric field at different times. The response time of the NP and the field-induced change in refractivity as a function of the laser peak intensity (bottom). (b) ATAS showing pump-induced optical density change ΔOD (top and left). Decomposition of the induced absorption coefficient into three physical components (bottom and left). Localized charge around the Ti atom (blue line), which closely follows the laser fluence change (red line) (top and right). Electron density dynamics during the laser cycle (bottom and right). Here, (a) and (b) are adapted from Refs. [65,66], respectively.

With the attosecond polarization spectroscopy, Sommer *et al.* [65] investigated the laser-induced charge polarization in SiO_2, as shown in Fig. 4(a). The nonlinear polarization is found to have ~ 100 as response time and to cause a change in refractive index. The nonlinear polarization indicates the energy transfer between the field and material, which removes the electrons from equilibrium location when laser field is growing and releases them back and radiates a part of the energy when the field decreases. The distribution of electron density within sub-fs reveals that

the electrons located in the vicinity of the oxygen atoms dominate the polarization response, whereas the electron cloud around the silicon centres remains largely unaffected.

Similar reflectivity modulation by strong laser field is also observed recently.[67] The electronic delay time is revealed to vary from 425 ± 98 to 575 ± 45 as, depending on the driver-field strengths. The phase delay is attributed to the increase of excitation carrier density, the Stark effect, and the system's polarizability, which is modulated by the synthesized light waveforms.

Another attractive issue in the community is the screening dynamics of electrons. Although the APS has been used to studied the attosecond dynamics in transition metal elements,[51,54] the electronic perturbation or screening effect induced by the optical field is completely neglected. The mechanism of light-induced screening dynamics for correlated electrons, such as *d*-orbital electrons, is still unclear.

To bridge this gap, Volkov *et al.*[66] combined the sensitivity of intra-shell transitions to screening effects[68] with the attosecond resolution to uncover the interplay of photo-absorption and screening in the transition metals Ti and Zr. The electrons are excited by the NIR laser and probed by the XUV pulse. The pump-probe spectrogram displays no induced transparency features, as shown in Fig. 4(b), indicating that the expected state-filling effect is completely canceled by a many-body phenomenon. Based on the time-dependent density functional theory (TDDFT) simulations, a *d*-orbital-shape build-up of the charge density has been identified at the end of the pulse, indicating a light-induced inflow of electron density towards the Ti atom which localizes on the *d* orbitals. The modified electron interaction also influences the core–hole lifetime by the super-Coster–Kronig Auger decay.

Interestingly, this screening dynamics exhibits strong element dependence even within the same compound and can be resolved by ATAS, as shown by Schumacher *et al.*[69] Their dynamic measurements on carrier dynamics following photoexcitation in $MoSe_2$ exhibit a many-body character for the carriers of the Mo atom, while the dynamics probed on the Se atoms remains entirely unaffected by such many-body interactions. Such unexpected contrast can be explained by a strong localization of photoexcited electrons around Mo atoms, which modifies the local field acting on the carriers. Moreover, the localization effects in gaped $MoSe_2$ live longer than those in Ti metal, due to the much higher e–e scattering rates in metals. The attosecond polarization and screening dynamics discussed above indicate that the many-body interactions efficiently modulate the ultrafast light–matter interactions as well as the electronic properties.

Attosecond Exciton Dynamics. The dynamic response of excitons in solids is central to modern condensed matter physics and photonic technologies.[70–73] The electro-optical properties of most semiconductors and insulators of technological interest are dominated by the excitons, while a clear observation of attosecond exciton dynamics is missing.

One of the pioneering works in this field was carried out by Moulet *et al.*[74] They combined an attosecond soft x-ray pump pulse with an attosecond optical probe to investigate the quasiparticle character and dynamics of excitons in SiO_2. The Stark shift and exciton bleaching are observed and used to identify the *s*- and *d*-like exciton states. The coupling between excitons and longitudinal (LO) phonons, the polarizability as well as the exciton radius are also measured by the near-edge spectroscopy.

As a quasiparticle composed of e–h pairs, the exciton typically has atom-like features and is well described by the Hydrogen atom model. However, by investigating the slow and fast components of the exciton relaxation in MgF_2 via the ATRS, Lucchini *et al.*[75] revealed the solid-like characteristics of exciton which are non-negligible at the attosecond timescale. As shown in Fig. 5(a), the slow component of exciton relaxation shows a few-fs dynamics, which originates from optical Stark effects due to a shift of exciton energy levels, indicating a typical atom-like character. In contrast, the fast component shows clear oscillations with a V-shaped dispersion in the time-frequency spectra. The V-shaped dispersion was found to result from the DFKEs, which has been observed in diamond,[44,76] suggesting a clear link between the exciton dynamics and attosecond intraband motion of virtual charges. The energy of the e–h particles follows the carriers of conduction state and exhibits a parabolic profile, which confirms the solid-like characteristics of these excitons.

More importantly, the long-range Coulomb interactions of excitons have been revealed to affect the motion of delocalized carriers, directly in the time domain, as Freudenstein *et al.*[77] investigated in Fig. 5(b). They managed to prove this via directing the e–h pair recollision in WSe_2 under intense THz fields and detecting them though the high-order sideband (HSB) radiation. The results reveal that by changing coherence between e–h pairs, many-body Coulomb correlations such as excitonic binding modify the trajectories and recollision times, leading to a shift of recollision timing by up to 1.2 ± 0.3 fs in atomically thin WSe_2 as compared to the bulk material.

With circularly polarized NIR pulses σ^- and σ^+ to selectively populate the opposite $\boldsymbol{K}$ and $\boldsymbol{K}'$ valleys, the many-body correlations also leave characteristic timing imprints since the valley polarization can be exploited to switch the strength of the Coulomb interaction between electrons at wave vectors $\boldsymbol{K}$ and $\boldsymbol{K}'$.[78,79] As a result, the e–h pairs generated by σ^- (σ^+) excitation during the positive (negative) half-cycles of the driving field yield stronger HSB than that generated during the half-cycles of opposite polarity.

Attosecond Magnetization Dynamics. Despite more than 20 years of development, the underlying physics of the laser-induced magnetization dynamics is still ambiguous and in debate. For example, what is the coupling mechanism among spin, orbital, charge, and light? How do these couplings affect the magnetic dynamics within a few hundreds of attoseconds of photoexcitation? The interactions of ultrafast laser with magnetic materials not only have potential applications in information technology, but also matter in basic science such as ultrafast demagnetization process, the optically generated spin current,[80,81] laser-induced spin reorientation,[82,83] and spin flip in com-

plex structures.[84–86] These aspects have been discussed in a recent review article.[87]

Notably, the first puzzling issue necessary to be clarified may be the dynamic mechanism of ultrafast demagnetization, which has been observed and studied over decades.[88] By performing real-time TDDFT simulations together with the Landau–Lifshitz–Gilbert model calculations, Chen *et al.*[89] investigated the dynamic mechanism in ferromagnetic Ni systems on the attosecond timescale. As shown in the two top panels of Fig. 6(a), they found a remarkable change of orbital angular momentum within the duration of light, due to electronic excitations. After 400 as, the light is turned off, the total angular momentum is conserved. A big exchange of the angular momentum between electron orbitals and ions is found. Meanwhile, some of the angular momentum has been transferred to the spin subsystem due to SOC. Their results reveal that the electrons and ions, as well as the spin and orbital degrees of freedom can exchange angular momentum in an ultrafast rate (hundreds of attoseconds), due to the strong interactions among light, orbital, spin, and nuclei.

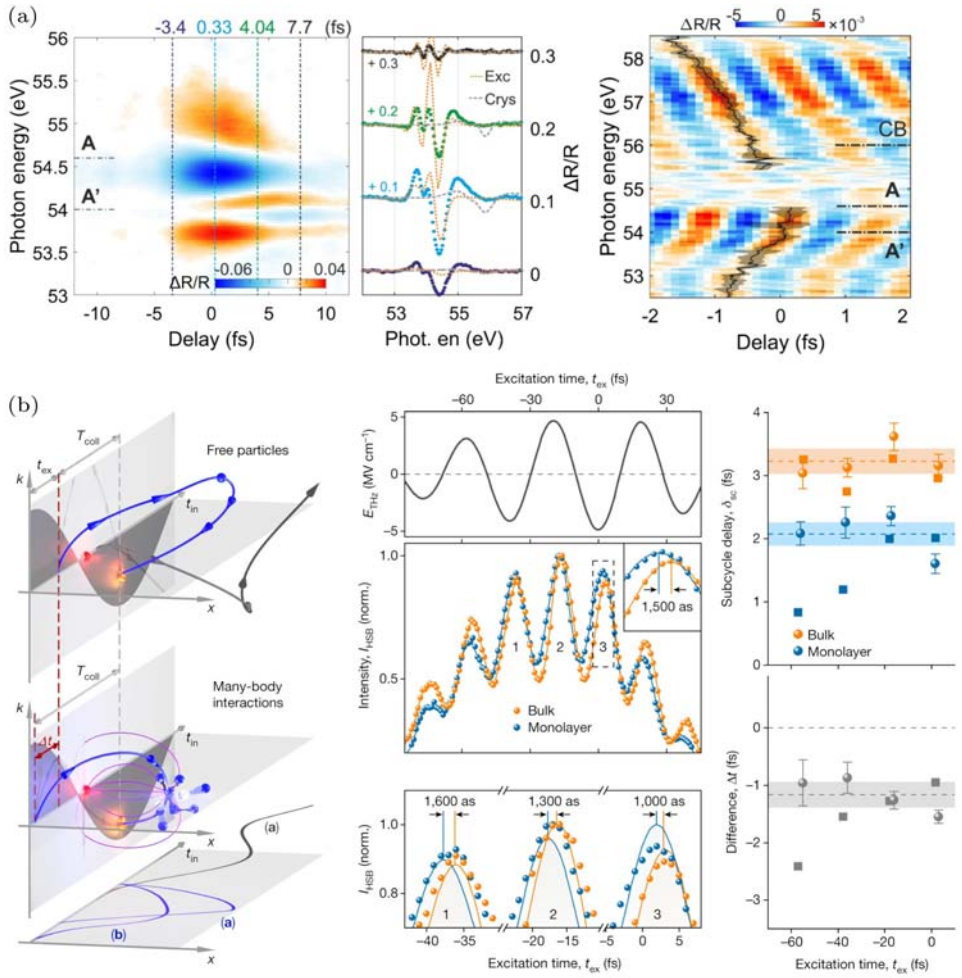

Fig. 5. (a) Slow component of experimental transient reflection $\Delta R/R$ spectrograms as a function time (left). Measured (dots) and calculated (dotted and dashed curves) $\Delta R/R$ profiles for four representative delays (middle). Fast component of the experimental $\Delta R/R$ (right). (b) Schematic phase-space trajectories of e–h pair emitting high-order sideband (HSB) radiation (left). Experimentally recorded THz driving field, spectrally integrated HSB intensity, in bulk (orange) and monolayer WSe_2 (blue) as a function of time delay (middle). Measured (spheres) and computed (squares) subcycle delay in bulk (orange) and monolayer (blue) WSe_2 (right). Here, (a) and (b) are taken from Refs. [75,77], respectively.

Contrasting to the demagnetization is the problem whether and how can laser generate magnetism, especially at the attosecond scale. Theoretically, the work by Neufeld *et al.*[90] explored an ultrafast light-driven spin dynamics in a highly non-resonant and strong-field regime. They predicted that the nonmagnetic material such as BiH or H-$MoTe_2$ can transiently transform into a magnetic one via dynamical nonlinear spin-flip processes, which occur on attosecond timescales and are mediated by cascaded multi-photon and spin–orbital interactions [two bottom panels of Fig. 6(a)]. This laser-induced magnetization can transiently oscillate with a high frequency (e.g., at $\sim$100 as) even for linearly polarized driving, whose speed can be tuned by the laser power and wavelength. This response is enabled by transverse laser-driven currents in solids, and typically occurs on the timescale of $\sim$500 as.

Experimentally, critical for attosecond magnetism is a scheme with the ability to control and detect the attosec-

ond evolution of electronic excitations, combined with simultaneous observation on modifications of the magnetic moments of individual constituents of the sample. Florian *et al.*[91] took a pioneering step in this field, by linking ATAS with simultaneous attosecond time-resolved magnetic circular dichroism. As shown in Fig. 6(b), they succeeded in manipulating the magnetic properties of a ferromagnetic layer stack directly by the temporal evolution of laser electric field. The electronic excitations induced by ultrafast NIR laser in nickel sandwiched between platinum layers result in the local displacement of charge carriers across the layer interfaces,[80] from the states of nickel into vacant platinum states. With a crucial SOC, the displacement of charge induces spin and orbital momentum transfer, which modifies the spin moments of different layers. The magnetic response time is within 500 as, which is reduced by two orders of magnitude.

It is worth pointing out that these findings are surprising and even disruptive, since in common expectations, the magnetic properties of matter can only be affected indirectly by laser and on much longer timescales, owing to the lack of first-order interaction between light and spin. The above-mentioned attosecond studies linked directly the temporal evolution of the laser field to modulation of the spin moments, which prove the ultrafast coupling between light and magnetic moment of orbitals or spins at the attosecond scale, bringing new properties and new physics to the science of magnetic materials.

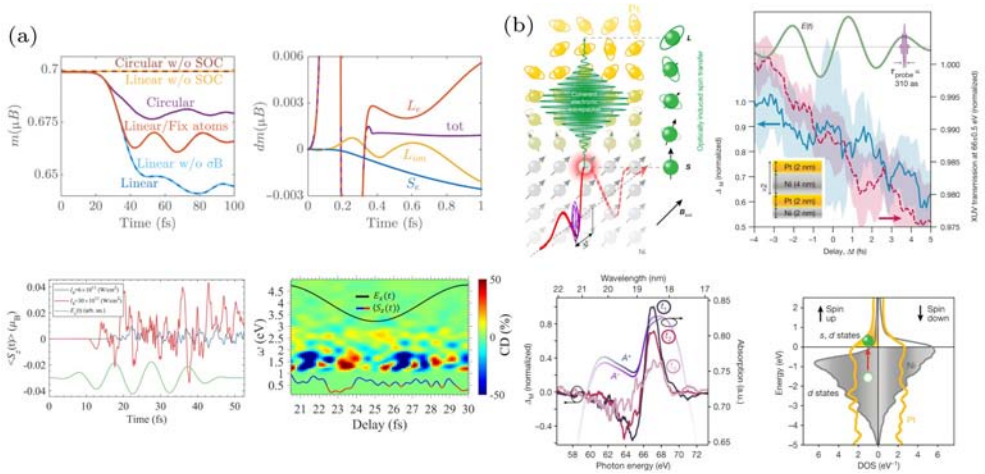

Fig. 6. (a) Evolution of magnetic moment per atom for Ni in different cases (top and left). Change of electron spin angular momentum, electron orbital angular momentum, ion angular momentum, and their total angular momentum for Ni (top and right). Change of electron spin angular momentum for BiH driven by a linearly polarized pulse (bottom and left). Attosecond-resolved circular dichroism (CD) in the linear driving case (bottom and right) for BiH. (b) Schematics showing the photoexcited spin-transfer mechanism across the interface between Ni (grey) and Pt (yellow) (top and left). Recorded absorption A^+ and A^- for the two orientations of the magnetic field and the resulting attosecond magnetic circular dichroism (MCD) signals contrast, at different excitation stages (bottom and left). Schematics showing the heteroatomic spin transfer mechanism in Ni–Pt multilayers (bottom and right). Transient MCD contrast (blue) and XUV transmission (red) measured in a Ni–Pt multilayer sample (top and right). Here (a) and (b) are taken from Refs. [89–91].

4. Attosecond Electronic Metrology and Data Encoding. The growing demand for unprecedented speeds and capacities in information society has been creating challenges in signal processing technology based on modern semiconductor photonics and electronics. However, the photonic/electronic devices at present rely on radiofrequency electric fields to control the physical properties of a semiconductor,[92] which limits their operating speed to THz frequencies.[93] This mismatch calls for laser-induced attosecond dynamics, which can be effectively tuned by complex synthesized light waveforms, a prospective approach to enhance the electrical signal or switching speed to PHz regime and to realize the attosecond data encoding.

As partly discussed above, the photoexcited carriers are accelerated and decelerated following the shape of vector potential of the driving field, causing an instantaneous modulation in the electronic structure of the dielectric system,[94,95] which leads to the change of dielectric and optical properties and enables the ultrafast encoding in solids.[41,67,96–99]

Using single-cycle intense optical fields to drive electron motions in bulk SiO_2, and probing the dynamics by ASC,[100,101] Garg *et al.*[102] extended the electronic metrology to the multi-PHz frequency range. Their results reveal a firm link between the emission of the XUV radiation and the light-induced intraband currents. As shown in Fig. 7(a), the frequency of phase-coherent electric current reaches $\sim$ 8 PHz, which is approximately an order of magnitude higher than the earlier efforts.[96] The metrology also enables access to the dynamic nonlinear conductivity, which builds up within approximately 700 as and switches periodically every $\sim$ 30 as.

Very recently, via an attosecond light field synthesizer (ALFS),[103] Hui *et al.*[104] realized the optical reflectivity switches in fused SiO_2, which are reversible following the oscillation direction of driving field. As shown in Fig. 7(b), in 900 as time scale the reflectivity switches from the maximum (ON state) to the minimum (OFF state) with a $\sim$45% change of the total value, showing an ultrafast speed of 1.1 PHz. Moreover, using on-demand synthesized complex waveforms generated by ALFS, this transient modification can be controlled to engineer the signal waveform.

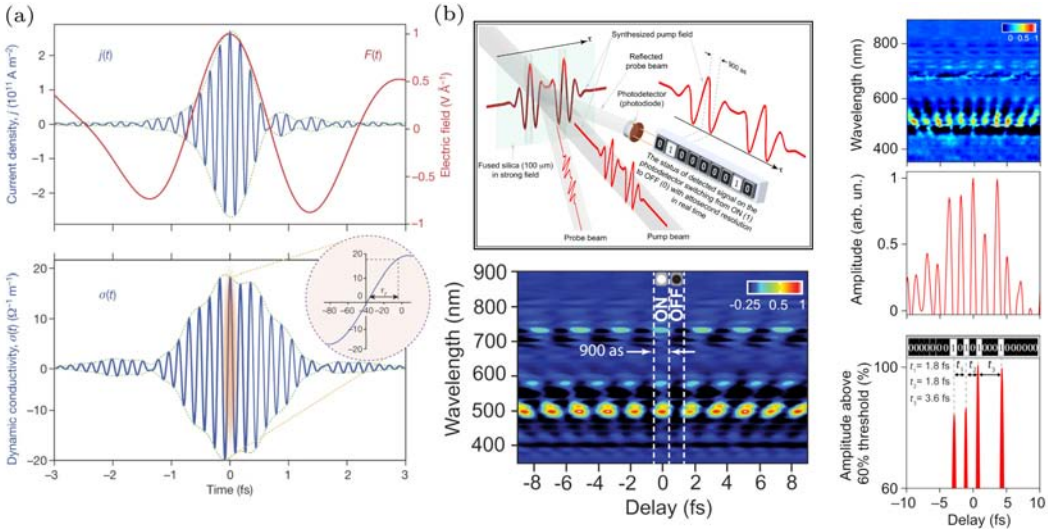

Fig. 7. (a) Nonlinear current density (blue curve) and driving optical field (red curve) as a function of time (top). Induced nonlinear dynamic conductivity as a function of time in SiO_2 (blue curve). Inset highlights the rapid switching of the conductivity within ∼30 as (bottom). (b) The basic principle of the attosecond optical switching based on the strong field interaction with dielectric (top and left). The spectrogram obtained by subtracting the probe spectrum in the absence of pump field from the measured spectrogram. The reflectivity switches between maximum to minimum alternatively in 900 as time scale (bottom and left). Ultrafast light field encoding (right). Here (a) and (b) are taken from Refs. [102,104], respectively.

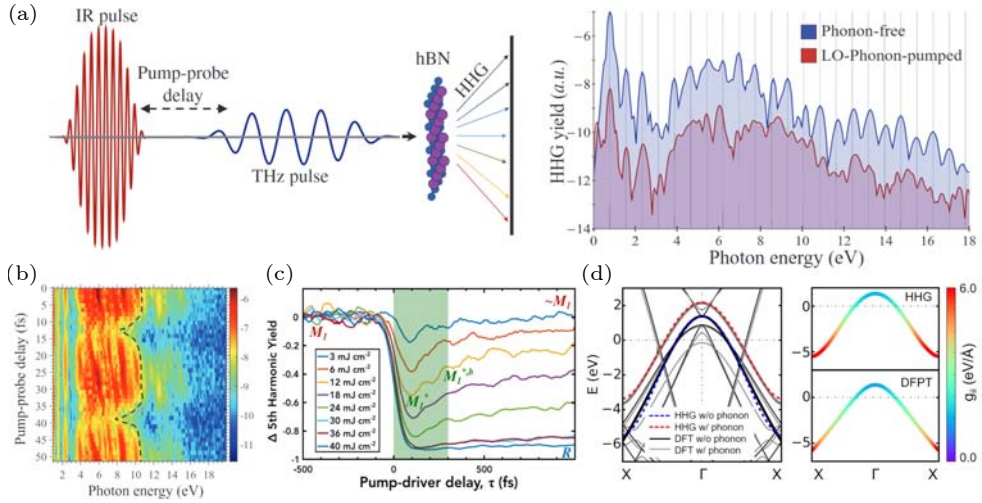

Fig. 8. (a) Schematics showing the pump-probe HHG setup for coherent phonons (CPs). The THz pulse is used to excite the phonons and the IR pulse is used to probe the phonon dynamics by generating HHG (left). HHG spectra with and without pre-excited LO phonon motion in hBN (right). (b) Temporally resolved HHG response with active LO phonons in hBN. (c) Temporally resolved intensity of 5^{th} HHG with phonons in VO_2. (d) The band structure (left) and the EPC matrix element g_{ii} (right) of LO phonon obtained by HHG reconstructions and DFT calculations in high-pressure superconductor H_3S. Here (a) and (b) are taken from Ref. [105], (c) and (d) from Refs. [106,107], respectively.

By setting a certain amplitude threshold, the number of the detected photon signals (above this threshold) and the switching time vary depending on the shape of the driving laser field.

5. Outlook. Various ultrafast pump-probe approaches, combined with advanced theories especially the state-of-art first-principles TDDFT calculations, have demonstrated their power to access the attosecond processes with multiple couplings in condensed matter. Interestingly, even at attosecond timescale, many-body interactions (including the electron–electron, electron–hole, electron–phonon, and spin–orbital interactions) in solids have already affected the dynamic mechanisms, which further induce new properties that are completely different from the ground state. We conclude with some perspectives on the future directions for ultrafast condensed matter physics at the attosecond timescale.

Towards Multi-Dimensional Attosecond Spectroscopy. The first agendum lies in expanding the multi-dimensional detection ability of attosecond spectroscopy to meet the measurement challenges in condensed matter physics.

Taking the HHG spectroscopy for instance, HHG spec-

troscopy can be further applied on complex samples and environments (such as heterojunction, liquid, and high-pressure states)[23] to obtained fundamental properties of solid in extreme conditions. One of the representative examples is the room-temperature superconductors under high pressure,[108,109] whose mechanism of superconductivity is not confirmed, due to the lacking of effective approach to probe the electronic band structure, even the ARPES loses its power under such high pressures. By contrast, the properties including vacuum free and non-restriction to electron occupation inspire HHG spectroscopy as a potential approach complementary to ARPES for band structure probing of high-pressure quantum states.

On the other hand, the effect of atomic dynamics on solid HHG is often ignored. This approximation rigidly separates the combined electron-nuclear dynamics, hindering the application of HHG to analyze phonon dynamics and NA effects on the attosecond electronic response in solids. This gap stands in stark contrast to gas-phase molecules, where the relationship between the nuclear autocorrelation function and HHG spectroscopy[110] has been revealed and applied to probe the electron-nuclear-coupled dynamics.[111,112]

As the community starts to realize very recently,[105–107,113] the temporal resolution of HHG needs to be well utilized to explore not only the phonon dynamics, but also the basic parameters including EPC. As shown in Figs. 8(a)–8(c), with the pump-probe setup, Neufeld *et al.* and Bionta *et al.* have demonstrated both theoretically and experimentally that the time-depended HHG spectra can be an effective approach to probe the phonon dynamics and lattice phase transitions.[103,104] In our recent study,[109] we theoretically propose that both the band structure and the EPC matrix element of the materials, e.g., the high-pressure superconductor, can be effectively probed by the HHG spectroscopy [Fig. 8(d)], which may be helpful for experimentally exploring the mechanism of room-temperature and high-pressure superconductivity in the near future.

Other issues include using the time-dependent HHG to detect the nuclear quantum effects, the electron coherence time as well as the time-resolved valence electron fluctuation under strong driving field, which are well studied in molecules while remain elusive in solids.

Entering the Fundamental Physics. The exploration on attosecond dynamics is uniquely positioned to provide new scientific insights on fundamental physics problems, such as the dynamic mechanism of quasiparticle formation and phase transition in condensed matter physics.

(i) HHG spectroscopy, whose intensity and cutoff energy are shown to be sensitive to the competition between the hopping and Coulomb repulsion of electrons,[114–116] is becoming a potential approach to study the strongly correlated systems,[117] as suggested by the recent exciting experiment in Mott insulator Ca_2RuO_4.[118] The attosecond investigation on screening dynamics suggests an effective estimation on the dynamic value of Hubbard U[119] experimentally, which can help to understand the long-debated mechanism of light-induced metal-insulator phase transition, for example, in VO_2.[120] It is also expected to be a probe to find out the mechanism when electron dynamics is approaching the quantum critical point.[121]

(ii) Although there are still some disputes,[122] HHG is also aimed to provide signatures for the topology of material. Recent experiments have reported[34,35] the novel behaviors of HHG relevant to the topological surface states. Theoretical studies also predict the role of shift vector on the time- and angle-dependent emissions of HHG dynamics.[123,124]

(iii) For exciton dynamics, on the other hand, the high temporal resolution of ATAS/ATRS can well separate the time scale of exciton formation/melting ($\sim$fs) and lattice dynamics ($\sim$ps),[125] which would contribute to determine the competition mechanism between excitonic insulator and CDW in 1T-$TiSe_2$ and Ta_2NiSe_5,[126–129] and even to estimate the time scale of exciton condensation.[130]

More interestingly, the recently discovered Kagome materials AV_3Sb_5 (A = K, Rb, or Cs),[131–133] where the flat band, Dirac cone and van Hove singularity coexist, have displayed the rich phase diagrams including the novel charge phases (CDW, pair density wave and electronic nematicity[134–136]), the topology and anomalous Hall effects,[137,138] the double-peak domain of superconductivity,[139,140] and antiferromagnet.[141] The sensitivity of attosecond dynamics to various microscopic degrees of freedom, as displayed previously, would help to uncover abundant dynamic mechanism behind these competitive and coexisting phases.

From Measurement to Manipulation. The universality and robustness of attosecond laser control paves a new way to functional material engineering. The precise control on light waveform generated by the ALFS enables the on-demand manipulation of materials. For example, the tailored polarization laser pulse has allowed researchers to create enantio-sensitive interferences for efficient chiral discrimination in ultrafast time scales.[142] In solids, more importantly, by a tailored light-wave driving, band structure engineering can be realized in attosecond timescale due to the time-reversal symmetry breaking, a resultant measurable valley Hall current can be detected via optical harmonic polarimetry.[143]

In summary, as a budding and active field, attosecond condensed matter physics will contribute more new scientific insights and inspiration to new scientific frontiers as well as conventional fields such as strong field physics and ultrafast material science. The relevant studies also pave the way for advanced science and technology in the future such as attosecond lasers, laser medical engineering, and ultrafast electronic devices.

Acknowledgements. This work was supported by the National Key Research and Development Program of China (Grant No. 2021YFA1400200), the National Natural Science Foundation of China (Grant Nos. 12025407, 92250303, and 11934003), and Chinese Academy of Sciences (Grant Nos. YSBR047 and XDB330301). We also acknowledge Xiang-He Feng and Yun-Zhe Jia for the assistance and constructive suggestions on writing. Shi-Qi Hu acknowledges financial support from the National Science Fund for Distinguished Young Scholars (Grant

No. 12304096), China Postdoctoral Science Foundation (Grant No. 2022TQ0362), and Special Research Assistant of Chinese Academy of Sciences Foundation.

References

[1] Maiman T 1960 *Nature* **187** 493
[2] Mankowsky R *et al.* 2014 *Nature* **516** 71
[3] Mitrano M *et al.* 2016 *Nature* **530** 461
[4] McIver J W *et al.* 2020 *Nat. Phys.* **16** 38
[5] Duan S F *et al.* 2021 *Nature* **595** 239
[6] Kogar A *et al.* 2020 *Nat. Phys.* **16** 159
[7] Zhang J *et al.* 2019 *Nano Lett.* **19** 6027
[8] Wang Y H *et al.* 2013 *Science* **342** 453
[9] Zhou S H *et al.* 2023 *Nature* **614** 75
[10] Pitruzzello G 2022 *Nat. Photon.* **16** 550
[11] He L X *et al.* 2022 *Chin. Phys. B* **31** 123301
[12] Hentschel M *et al.* 2001 *Nature* **414** 509
[13] Kienberger R *et al.* 2004 *Nature* **427** 817
[14] Sansone G *et al.* 2006 *Science* **314** 443
[15] Goulielmakis E *et al.* 2008 *Science* **320** 1614
[16] Zhao K *et al.* 2012 *Opt. Lett.* **37** 3891
[17] Thomas G *et al.* 2017 *Opt. Express* **25** 27506
[18] Sekikawa T *et al.* 2004 *Nature* **432** 605
[19] Mashiko H *et al.* 2008 *Phys. Rev. Lett.* **100** 103906
[20] Ferrari F *et al.* 2010 *Nat. Photon.* **4** 875
[21] Xue B *et al.* 2020 *Sci. Adv.* **6** eaay2802
[22] McPherson A *et al.* 1987 *J. Opt. Soc. Am. B* **4** 595
[23] Zong A *et al.* 2023 *Nat. Rev. Matter* **8** 224
[24] Geneaux R *et al.* 2019 *Philos. Trans. R. Soc. A* **377** 20170463
[25] Goulielmakis E *et al.* 2022 *Nat. Photon.* **16** 411
[26] Wu M X *et al.* 2015 *Phys. Rev. A* **91** 043839
[27] Vampa G *et al.* 2015 *Phys. Rev. B* **91** 064302
[28] Chin A H *et al.* 2001 *Phys. Rev. Lett.* **86** 3292
[29] Ghimire S *et al.* 2011 *Nat. Phys.* **7** 138
[30] Vampa G *et al.* 2015 *Phys. Rev. Lett.* **115** 193603
[31] Lanin A A *et al.* 2017 *Optica* **4** 516
[32] Lv Y Y *et al.* 2021 *Nat. Commun.* **12** 6437
[33] Luu T *et al.* 2018 *Nat. Commun.* **9** 916
[34] Bai Y *et al.* 2021 *Nat. Phys.* **17** 311
[35] Schmid C P *et al.* 2021 *Nature* **593** 385
[36] You Y *et al.* 2017 *Nat. Phys.* **13** 345
[37] Lakhotia H *et al.* 2020 *Nature* **583** 55
[38] Hu S *et al.* 2023 *Nat. Commun.* (submitted)
[39] Mashiko H *et al.* 2016 *Nat. Phys.* **12** 741
[40] Schlaepfer F *et al.* 2018 *Nat. Phys.* **14** 560
[41] Schultze M *et al.* 2013 *Nature* **493** 75
[42] Martin S *et al.* 2014 *Science* **346** 1348
[43] Emin D and Hart C F 1987 *Phys. Rev. B* **36** 7353
[44] Lucchini M *et al.* 2016 *Science* **353** 916
[45] Sidiropoulos T P H *et al.* 2021 *Phys. Rev. X* **11** 041060
[46] Ossiander M *et al.* 2018 *Nature* **561** 374
[47] Haynes D C *et al.* 2021 *Nat. Phys.* **17** 512
[48] Fabian S *et al.* 2017 *Science* **357** 1274
[49] Seth L C 2017 *Phys. Rev. X* **7** 041030
[50] Ito *et al.* 2023 *Nature* **616** 696
[51] Cavalieri A *et al.* 2007 *Nature* **449** 1029
[52] Garg M *et al.* 2022 *Nat. Photon.* **16** 196
[53] Nabben D *et al.* 2023 *Nature* **619** 63
[54] Tao Z S *et al.* 2016 *Science* **353** 62
[55] Heinrich S *et al.* 2021 *Nat. Commun.* **12** 3404
[56] Corkum P B 1993 *Phys. Rev. Lett.* **71** 1994
[57] Lewenstein M *et al.* 1994 *Phys. Rev. A* **49** 2117
[58] Schultze M *et al.* 2010 *Science* **328** 1658
[59] Kelkensberg F *et al.* 2011 *Phys. Rev. Lett.* **107** 043002
[60] Siu W *et al.* 2011 *Phys. Rev. A* **84** 063412
[61] Ranitovic P *et al.* 2014 *Proc. Natl. Acad. Sci. USA* **111** 912
[62] Calegari F *et al.* 2014 *Science* **346** 336
[63] Kraus P M *et al.* 2015 *Science* **350** 790
[64] Matselyukh D T *et al.* 2022 *Nat. Phys.* **18** 1206
[65] Sommer A *et al.* 2016 *Nature* **534** 86
[66] Volkov M *et al.* 2019 *Nat. Phys.* **15** 1145
[67] Hui D D *et al.* 2022 *Nat. Photon.* **16** 33
[68] Amusia M Y *et al.* 2000 *Rep. Prog. Phys.* **63** 41
[69] Schumacher Z *et al.* 2023 *Proc. Natl. Acad. Sci. USA* **120** e2221725120
[70] Krausz F *et al.* 2014 *Nat. Photon.* **8** 205
[71] Karni O *et al.* 2019 *Phys. Rev. Lett.* **123** 247402
[72] Novoselov K S *et al.* 2016 *Science* **353** aac9439
[73] Unuchek D *et al.* 2018 *Nature* **560** 340
[74] Moulet A *et al.* 2017 *Science* **357** 1134
[75] Lucchini M *et al.* 2021 *Nat. Commun.* **12** 1021
[76] Lucchini M *et al.* 2020 *J. Phys. Photon.* **2** 025001
[77] Freudenstein J *et al.* 2022 *Nature* **610** 290
[78] Xu X D *et al.* 2014 *Nat. Phys.* **10** 343
[79] Langer F *et al.* 2018 *Nature* **557** 76
[80] John K D *et al.* 2018 *Nano Lett.* **18** 1842
[81] Lambert C H *et al.* 2014 *Science* **345** 1337
[82] Kimel A *et al.* 2004 *Nature* **429** 850
[83] Le Guyader L *et al.* 2013 *Phys. Rev. B* **87** 054437
[84] Paolo C *et al.* 1993 *Phys. Rev. Lett.* **70** 694
[85] Cui L S *et al.* 2020 *Nat. Photon.* **14** 636
[86] Shankar S *et al.* 2018 *Nat. Commun.* **9** 4750
[87] Wu N *et al.* 2023 *Prog. Surf. Sci.* **2023** 100709
[88] Beaurepaire E *et al.* 1996 *Phys. Rev. Lett.* **76** 4250
[89] Chen Z H *et al.* 2019 *Sci. Adv.* **5** eaau8000
[90] Neufeld O *et al.* 2023 *npj Comput. Matter* **9** 39
[91] Siegrist F *et al.* 2019 *Nature* **571** 240
[92] Neamen D A 2011 *Semiconductor Physics and Devices: Basic Principles* (New York: McGraw-Hill)
[93] Mei X B *et al.* 2015 *IEEE Electron Device Lett.* **36** 327
[94] Tim P C *et al.* 2016 *Optica* **3** 1358
[95] Korobenko A *et al.* 2020 *Optica* **7** 1372
[96] Schiffrin A *et al.* 2013 *Nature* **493** 70
[97] Luu T *et al.* 2015 *Nature* **521** 498
[98] Husain A *et al.* 2022 *Faraday Discuss.* **237** 317
[99] Georg W *et al.* 2014 *Phys. Rev. Lett.* **113** 087401
[100] Itatani J *et al.* 2002 *Phys. Rev. Lett.* **88** 173903
[101] Goulielmakis E *et al.* 2004 *Science* **305** 1267
[102] Garg M *et al.* 2016 *Nature* **538** 59
[103] Husain A *et al.* 2022 *APL Photon.* **7** 041301
[104] Hui D D *et al.* 2023 *Sci. Adv.* **9** eadf1015
[105] Neufeld O *et al.* 2022 *Proc. Natl. Acad. Sci. USA* **119** e2204219119
[106] Bionta M R *et al.* 2021 *Phys. Rev. Res.* **3** 023250
[107] Hu S *et al.* 2023 arXiv:2304.09459 [cond-mat.mtrl-sci]
[108] Drozdov A P *et al.* 2015 *Nature* **525** 73
[109] Drozdov A P *et al.* 2019 *Nature* **569** 528
[110] Lein M 2005 *Phys. Rev. Lett.* **94** 053004
[111] Baker S *et al.* 2006 *Science* **312** 424
[112] Li W *et al.* 2008 *Science* **322** 1207
[113] Rana N *et al.* 2022 *Phys. Rev. B* **106** 064303
[114] Tikhomirov I D *et al.* 2017 *Phys. Rev. Lett.* **118** 203202
[115] Silva R E F *et al.* 2018 *Nat. Photon.* **12** 266
[116] Murakami Y *et al.* 2018 *Phys. Rev. Lett.* **121** 057405
[117] Imai S *et al.* 2020 *Phys. Rev. Lett.* **124** 157404
[118] Uchida K *et al.* 2022 *Phys. Rev. Lett.* **128** 127401
[119] Nicolas T D *et al.* 2018 *Phys. Rev. Lett.* **121** 097402
[120] Xu J Y *et al.* 2022 *Sci. Adv.* **8** eadd2392
[121] Shao C *et al.* 2022 *Phys. Rev. Lett.* **128** 047401
[122] Neufeld O *et al.* 2023 *Phys. Rev. X* **13** 031011
[123] Qian C *et al.* 2022 *Phys. Rev. X* **12** 021030
[124] Uzan-Narovlansky A *et al.* 2022 *Research Square*
[125] Rohwer T *et al.* 2011 *Nature* **471** 490
[126] Lian C *et al.* 2020 *Nat. Commun.* **11** 43
[127] Lin Z J *et al.* 2022 *Phys. Rev. Lett.* **129** 187601
[128] Lu Y F *et al.* 2017 *Nat. Commun.* **8** 14408
[129] Kim K *et al.* 2021 *Nat. Commun.* **12** 1969
[130] Wang Z *et al.* 2019 *Nature* **574** 76
[131] Brenden R O *et al.* 2019 *Phys. Rev. Mater.* **3** 094407
[132] Yin Q, Tu Z, Gong C, Fu Y, Yan S, and Lei H 2021 *Chin. Phys. Lett.* **38** 037403
[133] Chen X, Zhan X, Wang X, Deng J, Liu X B, Chen X, Guo J G, and Chen X 2021 *Chin. Phys. Lett.* **38** 057402
[134] Nie L P *et al.* 2022 *Nature* **604** 59
[135] Jiang Y X *et al.* 2021 *Nat. Mater.* **20** 1353
[136] Chen H *et al.* 2021 *Nature* **599** 222
[137] Brenden R O *et al.* 2020 *Phys. Rev. Lett.* **125** 247002
[138] Yang S Y *et al.* 2020 *Sci. Adv.* **6** eabb6003
[139] Zheng L X *et al.* 2022 *Nature* **611** 682
[140] Zhong Y Q *et al.* 2023 *Nature* **617** 488
[141] Teng X K *et al.* 2022 *Nature* **609** 490
[142] Laura R *et al.* 2022 arXiv:2206.01719 [physics.optics]
[143] Sambit M *et al.* 2023 arXiv:2303.13044 [cond-mat.mes-hall]